A Gas Sensor Array Using Carbon Nanotubes and Microfabrication Technology

Jing Li,*,z **Yijiang Lu, Qi Ye, Lance Delzeit, and M. Meyyappan****

NASA Ames Research Center, Center for Nanotechnology, Moffett Field, California 94035, USA

A nanosensor technology has been developed using single-walled carbon nanotubes (SWNTs) combined with silicon-based microfabrication processes. A sensor array containing twelve interdigitated electrode (IDE) pairs with different gap sizes has been designed. The IDE fingers were fabricated using photolithography and thin-film metallization techniques. SWNTs were grown directly on the IDEs for trace amounts of gas detection. This sensor array has been exposed to nitrogen dioxide at various concentrations from 10 ppm to 400 ppb, and ammonia from 50 to 5 ppm. The results show a very reproducible sensor performance from one sensor to the other in the array.
© 2005 The Electrochemical Society. [DOI: 10.1149/1.2063289] All rights reserved.

Monitoring concentrations of chemicals, gases, and vapors is a critical task in the chemical industry, power plants, automotive exhaust, environmental protection, planetary science, and numerous other situations. Chemical sensors for specific species with varying sensitivity and discrimination levels are commercially available. Common chemical sensors differ in terms of the sensing material and the nature of the property change (such as electrical conductivity, optical characteristics, temperature, etc.). Some of the current sensor technologies include high temperature oxide thin-film sensors, polymer-based sensors, catalytic-based sensors, and surface acoustic wave sensors.[1] Key attributes expected of a sensor include sensitivity in the parts per million to billion (ppm, ppb) range where trace levels are involved, absolute discrimination, room temperature operation, low power consumption, reasonable size, volume and mass, and low cost for large-scale applications. Given such a broad set of desirable attributes and diverse application fields, sensor development is a constantly evolving research area. The newest contributions to this field are nanoscience and technology where novel nanomaterials, because of their size, large surface to volume ratio, and properties that differ from their bulk counterparts, promise to offer better performance than micro- and macrosensors.

Some of the candidate nanomaterials include carbon nanotubes (CNTs),[2] inorganic nanowires of high-temperature oxides and semiconducting elements or compounds, and quantum dots. Of these, CNTs have commanded much attention for physical, chemical, and biosensors due to their interesting physical, electrical, and other properties.[3] The sensor array described in this article consists of carbon nanotubes as sensing material and an interdigitated electrode (IDE) as a transducer. It is one type of electrochemical sensor that depends on the transfer of charge from one electrode to another electrode. This means that at least two electrodes constitute an electrochemical cell to form a closed electrical circuit. Due to the curvature of the graphene sheet in single-walled carbon nanotubes (SWNTs), the electron clouds change from a uniform distribution around the C–C backbone in graphite to an asymmetric distribution inside and outside the cylindrical sheet of the nanotube.[2] Since the electron clouds are distorted, a rich π-electron conjugation forms outside the tube, therefore making the carbon nanotube electrochemically active. Electron donating and withdrawing molecules such as nitrogen dioxide (NO_2) and ammonia (NH_3) will either transfer electrons to or withdraw electrons from SWNTs, thereby giving SWNTs more charge carriers, either electrons or holes respectively, which increases or decreases the nanotube conductance accordingly.[4,5] Theoretical calculation showed the binding energy of

the NO_2 and NH_3 to carbon nanotubes,[6] which indicates that a weak charge transfer can occur. The typical electrochemical interaction may be denoted as

$$CNT + Gas \longrightarrow CNT^{\delta e}\ Gas^{\delta+}\ or\ CNT^{\delta+}\ Gas^{\delta e}$$

where δ is a number that indicates the amount of charge transferred during the interaction. The conductivity change may also be caused by the contact modulation between the metal electrode and carbon nanotube, and/or the contact between carbon nanotube and carbon nanotube. By measuring the conductivity change of the CNT device, the concentration of the chemical species or gas molecules can be measured. In this work, we describe a chemical sensor based on such a conductivity change using SWNTs. While carbon nanotubes can provide the sensitivity and other attributes expected from nanomaterials in general, broad commercial acceptance would largely depend on the ability for mass production and cost since the sensor market is extremely cost sensitive. Here, we also describe a microfabrication approach to fabricate the sensor platform incorporating the nanotubes.

A multilayer sensor array chip was designed and fabricated for optimal gas sensing capabilities with in situ heating and temperature monitoring. A detailed chip configuration schematic is shown in Fig. 1. p-Type boron-doped silicon(100) wafers with a resistivity of 0.006–0.01 Ω cm and thickness of 500 ± 25 μm were used as substrates. A layer of 0.5 μm silicon dioxide was thermally grown on top of the Si substrates. Patterned platinum (200 nm thick) lines were deposited on top of the SiO_2 layer for electrical heating and resistive temperature detection (RTD). A layer of 1 μm silicon nitride was deposited on top of the heaters and the RTDs as the insulating layer between the platinum heating elements and the IDE fingers. A layer of 200 nm platinum on top of 20 nm titanium was deposited on the Si_3N_4 layer onto the designed finger patterns. These patterns consisted of 4, 8, 12, and 50 μm finger gaps with 10 and 20 μm finger widths (see Fig. 1b).

Next, SWNTs need to be deposited on the surface of the IDEs. In our previous single-sensor efforts,[7] we have used a solution casting approach from bulk SWNT samples but here we have chosen an in situ chemical vapor deposition (CVD) process to deposit the SWNTs. The SWNT growth process and characterization are described in detail in Ref. 8 and only a brief outline is given here. The catalytic metals used in these experiments for SWNTs growth are 99.9% pure and are sputtered using a VCR Group Incorporated ion beam sputter (IBS), model IBS/TM200s. The deposition of the metal catalyst for growing SWNTs was over the entire area of the IDE fingers. The catalyst used to grow the SWNTs consists of two components, a metal underlayer (Al) and an active catalyst (Fe). Since the thin aluminum layer breaks up into droplets at the growth temperature, this layer does not form the conducting bridge between the two terminals. The Al underlayer helps to increase the nucleation and generation of the catalyst particles. The thickness of the Al underlayer was varied from 1 to 10 nm and the Fe catalyst was var-

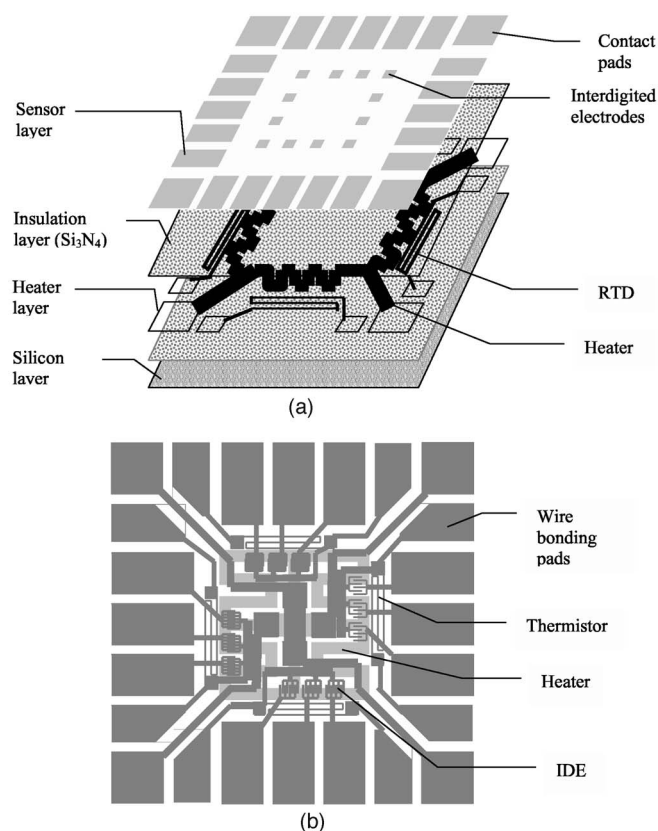**Figure 1.** (a) Schematic of the microfabrication process and various layers, (b) 1 cm × 1 cm chip with twelve sensor elements.

Table I. Characteristics of sensor-array-layered structure.

Properties	Si_3N_4 (Rauschert, Co.)	SiO_2 (Diamond Engineering)
Resistivity (Ω cm)	10^{14}	10^{16}
Thermal conductivity (W/m-k)	18	1.4
Thermal diffusivity (cm^2/s)	0.32	0.006
Thermal expansion coefficient (k^{-1})	2.9×10^{-6}	0.5×10^{-6}
Specific heat (J/g-k)	0.5	1.0

the heating layer and the IDE layer. Since Si_3N_4 has ten times higher thermal conductivity and fifty times higher diffusivity than SiO_2, Si_3N_4 can transfer heat from the heating layer more effectively to the top IDE layer. Platinum was chosen as the electrode material mainly due to its noble properties and higher melting point than gold for direct growth of SWNTs.

The density of the SWNTs across the IDE fingers can be controlled by the ratio of Fe to Al and the finger gap size (4–50 μm). Figure 2 shows scanning electron microscopy (SEM) images of SWNTs bridging the electrodes. It can be seen from Fig. 2b that the SWNT is in good contact with the platinum electrode. The *I-V* characteristics of all the devices were measured (not shown here) and found to yield acceptable resistance for sensor operation at 4 and
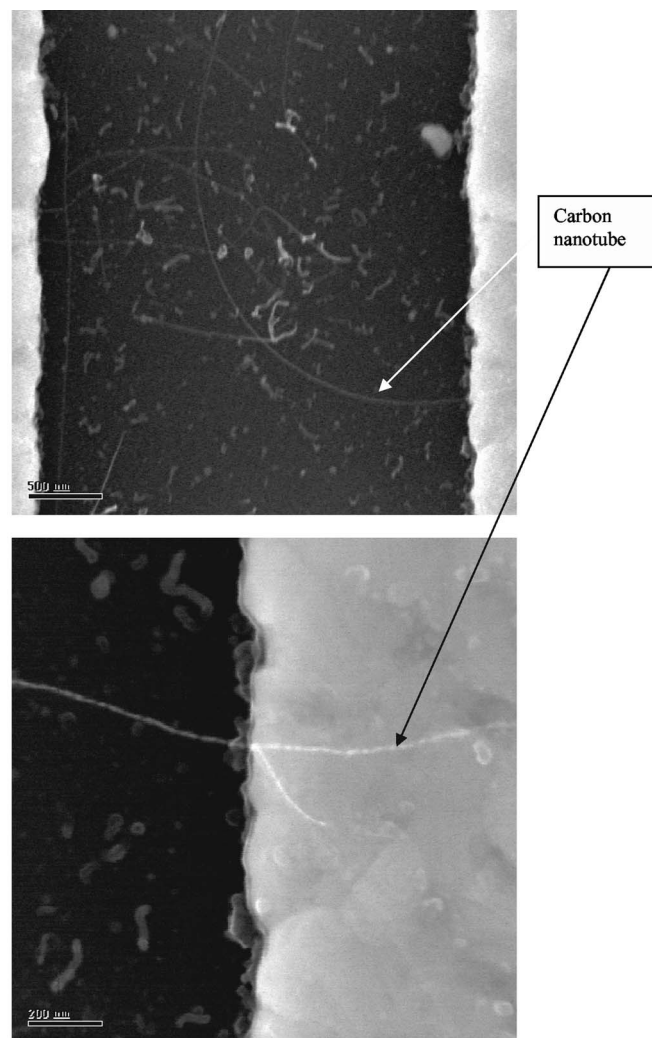
ied from 0.2 to 1.0 nm, by setting the deposition current on the IBS that corresponds to the thickness of the sputtered metal layer. A methane feedstock (1000 sccm) was used for a 10 min growth and the SWNT density was controlled by varying the Al and Fe layers to optimize the resistance and electrical signal. The fabricated sensor array chips were tested using a data acquisition card (DaqBoad/2000, IOtech, Inc., Cleveland, OH) and an adapter board (DBK203, IOtech, Inc., Cleveland, OH) with screw terminals, also connects DBK signal conditioning and expansion options to a CA-195 expansion cable. A readout chip, separate from the sensor array chip, containing a Wheatstone bridge readout circuitry, was built to boost and massage the electrical signals from the sensor through the data acquisition card. This circuitry measured the voltage shift from the original excitation voltage when the gas was exposed to the sensor. Three channels were multiplexed during the measurement.

The fabricated sensor array chips were exposed to nitrogen dioxide and ammonia at various concentrations using a computerized multicomponent gas blending and dilution system, Environics 2040 (Environics, Inc., Tolland, CT). It created different concentration streams with a steady output flow of 400 cm^3/min during both exposure and purge periods. Air was used as the purge and the balance gas.

First, the test results show that the platinum wires in this sensor array layered structure provide good RTD. The plot of resistance vs temperature (not shown here) shows a linear relationship with a regression factor R^2 of 0.998 in the range of 50–300°C. The Si_3N_4 layer provides a pinhole-free layer with low stress at room temperature and at temperatures below 300°C. It also has high thermal shock resistance and high corrosion and wear resistance. Compared with SiO_2 (Table I), Si_3N_4 is a good interlayer material in between the heating layer and IDE layer. Both Si_3N_4 and SiO_2 are good electrical insulators that can prevent the electrical shortage between

Figure 2. SEM images of in situ growth of carbon nanotubes across two metal electrodes in a sensing element.
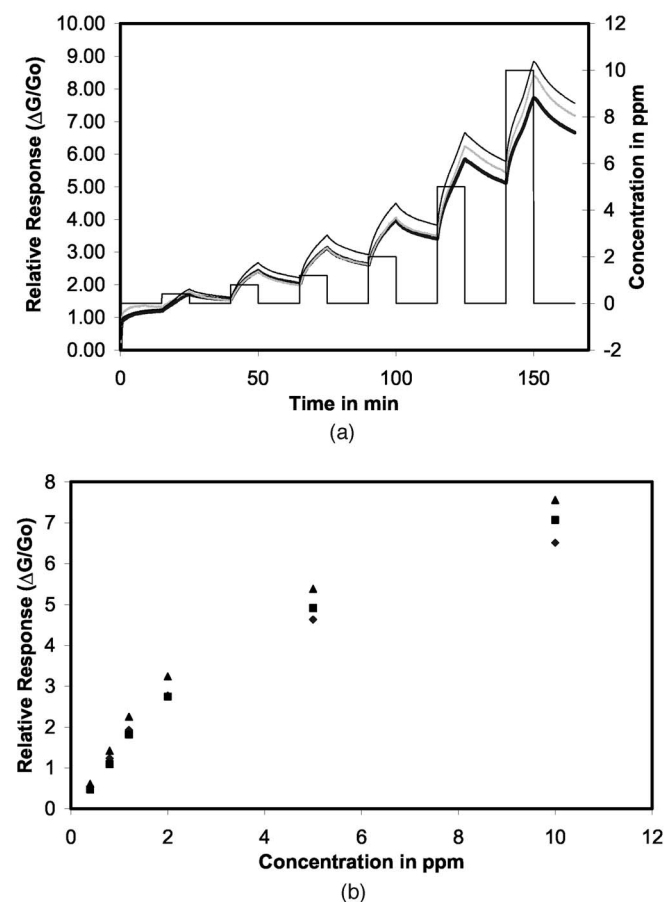
(a)

(b)

Figure 3. Sensor response to NO_2 vs (a, top) time and (b, bottom) concentration in room temperature (NO_2 was balanced with air, and the sensors were purged by air with a total flow rate of 400 cm³/min).

Figure 4. Sensor response to NH_3 in room temperature (NH_3 was balanced with air and the sensors were purged by air with a total flow rate of 400 cm³/min).

selectivity of the carbon nanotube sensors, such as coating the carbon nanotubes with different polymers[10] or doping the carbon nanotube with different metal clusters.[11,12]

In summary, we have used a conventional microfabrication approach to fabricate a sensor array in which SWNTs form the conducting channel or sensor element. The large surface area and other interesting electronic properties of SWNTs make them ideal for developing chemical sensors. The charge transfer between the nanotubes devices and gas molecules such as NO_2 and NH_3 leads to a reproducible conductivity change which forms the basis for the sensor operation. We have developed an array with twelve sensors which show a highly reproducible performance from sensor to sensor. The sensitivity level for NO_2 is 1 ppb and for NH_3, 125 ppb, based on the data in this work. Based on these results, we have developed a system for flight testing aboard a Lockheed-Martin Atlas V rocket. This system is expected to be useful in cosmochemistry applications as well as in several commercial and industrial applications.

50 μm gaps for given SWNT densities. Figure 3 shows the sensor response when the sensor array was exposed to nitrogen dioxide at various concentrations in air and sensors were purged by air with a total flow rate of 400 cm³/min. The dosage was 400 ppb, 800 ppb, 1.2, 2, 5, and 10 ppm at the intervals shown in Fig. 3. SWNTs respond to NO_2 exposure as expected, but the sensor response time along with the recovery time (i.e., the time it takes for the sensor to return to the baseline when the gas source is taken away) is slow. It is possible to accelerate the recovery time by exposing the sensor to UV light[9] (or by heating a little) which increases the rate of NO_2 desorption. Figure 3 shows the response of three random sensors out of the twelve in the array and, within experimental error, these sensors provide a reproducible performance. A plot of sensor response vs concentration shows a linear slope at low concentration levels and extrapolation of this linear region yields a sensitivity level of 1 ppb for NO_2 detection.

Figure 4 shows the response of the sensor array when exposed to NH_3 at various concentrations in air and sensors were purged by air with a total flow rate of 400 cm³/min. Here, in relative terms, the sensor recovery time is faster compared to NO_2 sensing. Again, three random sensors in the array show a very reproducible performance.

The carbon nanotube sensing devices provide opposite polarities of sensor signals from NO_2 and NH_3 exposures. Surface and bulk modifications of carbon nanotubes can be utilized to improve the
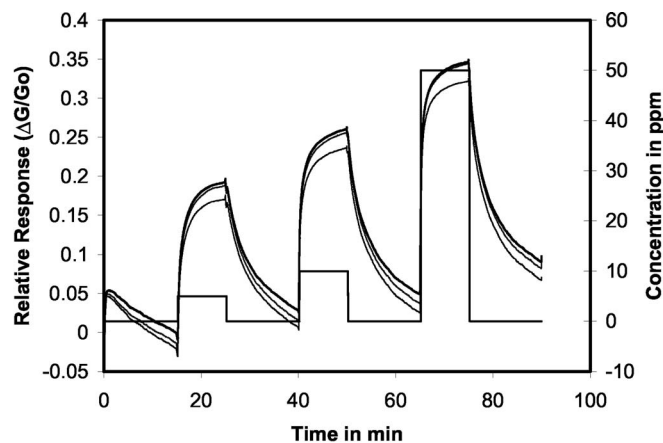
References

1. J. Janata, *Principles of Chemical Sensors*, Plenum Press, New York (1989).
2. *Carbon Nanotubes: Science and Applications*, M. Meyyappan, Editor, CRC Press, Boca Raton, FL (2004).
3. J. Li, in *Carbon Nanotubes: Science and Applications*, M. Meyyappan, Editor, CRC Press, Boca Raton, FL (2004).
4. C. K. W. Adu, G. U. Sumanasekera, B. K. Pradhan, H. E. Romero, and P. C. Eklund, *Chem. Phys. Lett.*, **337**, 31 (2001).
5. G. U. Sumanasekera, C. K. W. Adu, S. Fang, and P. C. Eklund, *Phys. Rev. Lett.*, **85**, 1096 (2000).
6. J. Zhao, A. Buldum, J. Han, and J. P. Lu, *Nanotechnology*, **13**, 195 (2002).
7. J. Li, Y. Lu, Q. Ye, M. Cinke, J. Han, and M. Meyyappan, *Nano Lett.*, **3**, 929 (2003).
8. L. Delzeit, B. Chen, A. M. Cassell, R. Stevens, C. Nguyen, and M. Meyyappan, *Chem. Phys. Lett.*, **348**, 368 (2001).
9. R. Chen, N. Franklin, J. Kong, J. Cao, T. Tombler, Y. Zhang, and H. Dai, *Appl. Phys. Lett.*, **79**, 6951 (2001).
10. J. Li, Y. Lu, and M. Meyyappan, *IEEE Sens. J.*, Submitted.
11. P. Young, Y. Lu, R. Terrill, and J. Li, *J. Nanosci. Nanotechnol.*, **5**, 1 (2005).
12. Y. Lu, J. Li, J. Han, H.-T. Ng, C. Binder, C. Partridge, and M. Meyyappan, *Chem. Phys. Lett.*, **391**, 344 (2004).